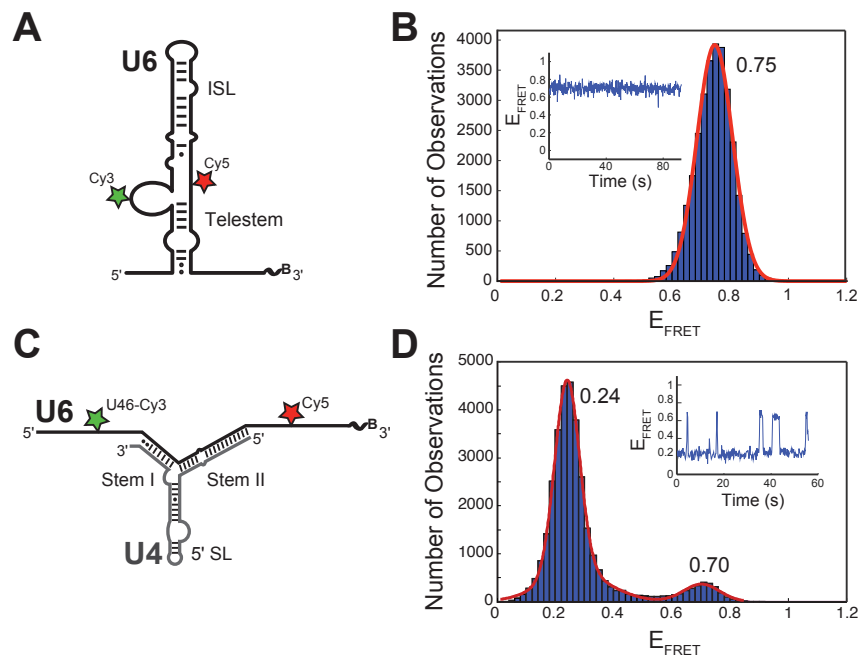


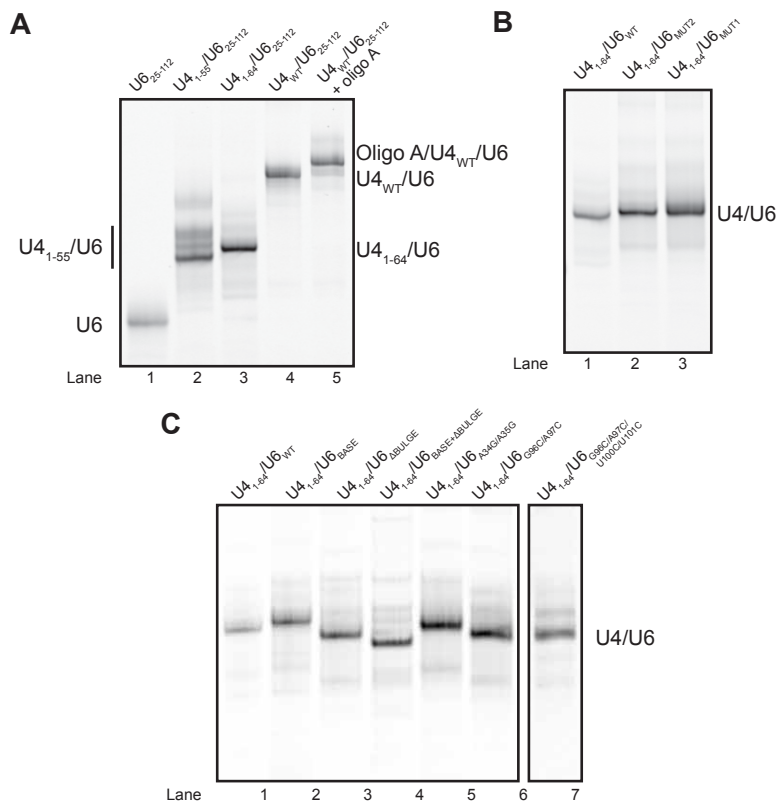
Supplemental Information for:

A Multi-step Model for Facilitated Unwinding of the Yeast U4/U6 RNA Duplex

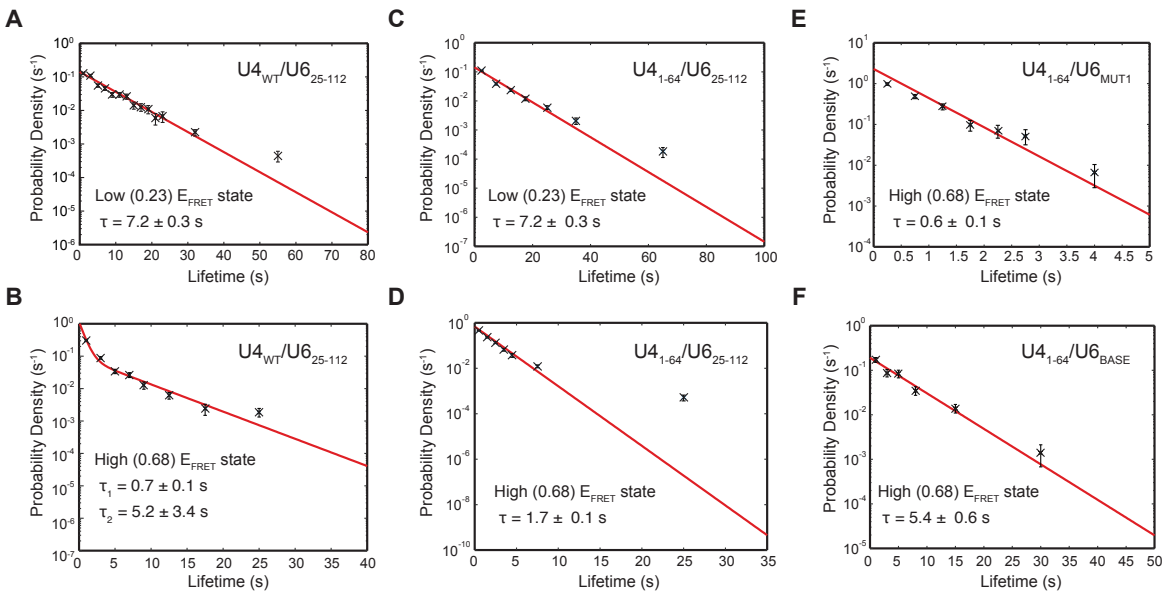
Margaret L. Rodgers, Allison L. Didychuk, Samuel E. Butcher, David A. Brow, and Aaron A. Hoskins



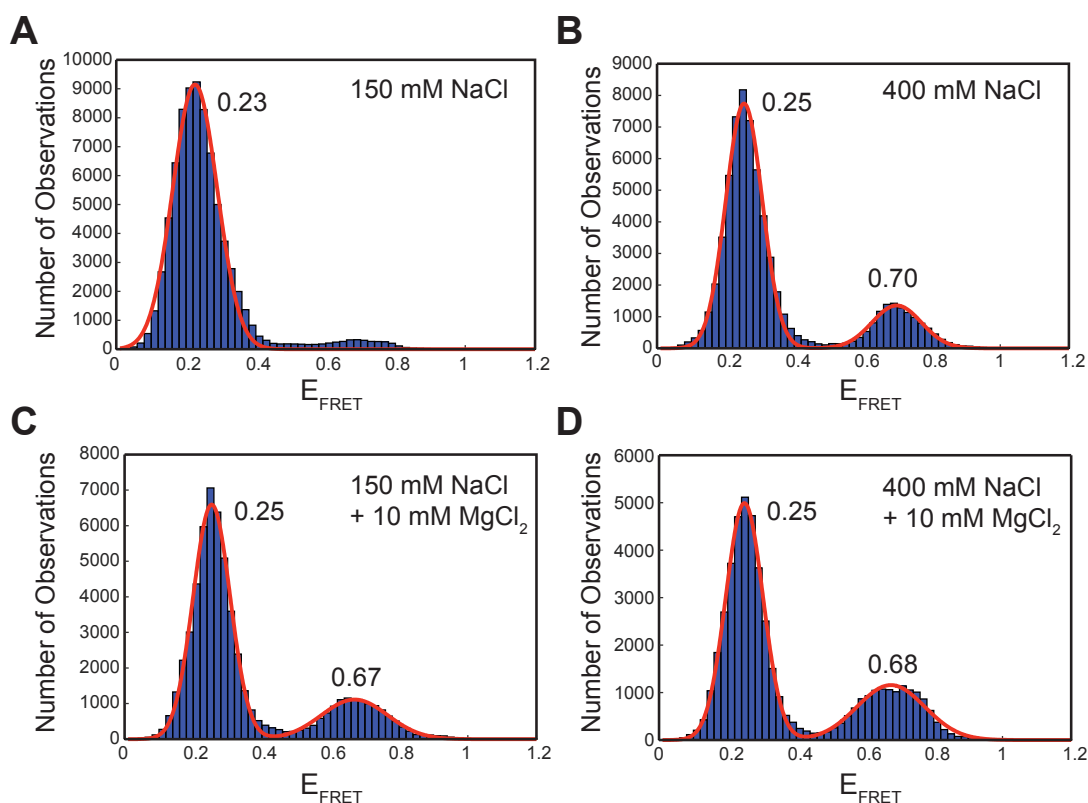
Supplemental Figure 1. U6 RNA labeled at U46 exhibits similar smFRET behaviors to RNAs labeled at U54. **(A)** Cartoon of the U46-labeled U6 RNA construct (U6₂₅₋₁₁₂) used in smFRET assays. FRET donor (Cy3) and acceptor (Cy5) fluorophores are denoted by green and red stars, respectively. **(B)** Histogram of E_{FRET} values obtained from single molecules of U46-labeled U6₂₅₋₁₁₂ ($N = 100$). The distribution could be fit to a single Gaussian function centered at 0.75 ± 0.01 (red line). No dynamics were observed in single molecule E_{FRET} time trajectories (*inset*). **(C)** The U46-labeled U4_{WT}/U6₂₅₋₁₁₂ diRNA used in smFRET assays. **(D)** Histogram of E_{FRET} values obtained from single molecules of U46-labeled U4_{WT}/U6₂₅₋₁₁₂ ($N = 121$). The distribution could be fit to a sum of two Gaussian functions centered at 0.24 ± 0.01 and 0.70 ± 0.01 (red line). Dynamics consistent with a reversible two-state conformational transition were apparent in single molecule E_{FRET} time trajectories (*inset*).



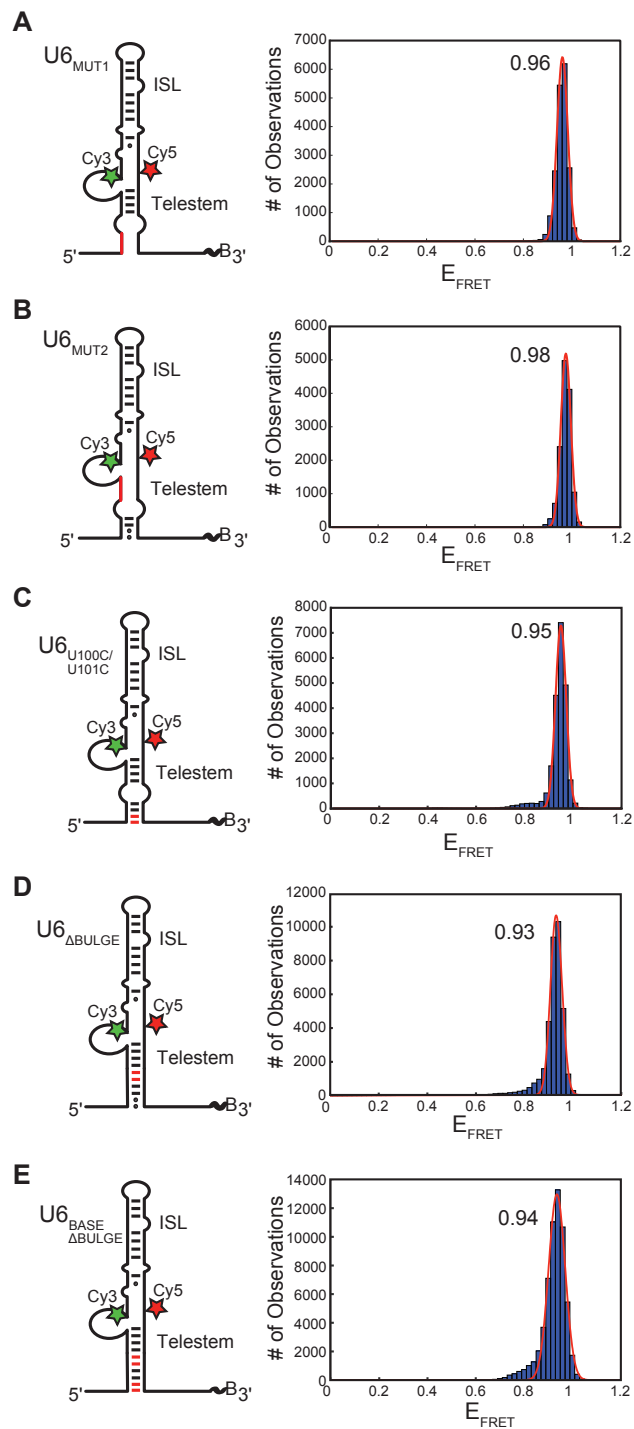
Supplemental Figure 2. Native gel analysis of complex formation between fluorescent U6 and non-fluorescent U4 RNAs. RNAs were analyzed by 6% nondenaturing PAGE and gels directly imaged by fluorescence. **(A)** Complex formation between U6₂₅₋₁₁₂ and U4₁₋₅₅ (lane 2), U4₁₋₆₄ (lane 3), and U4_{WT} (lane 4). The U4₁₋₅₅/U6 complex migrates heterogeneously, possibly due to multiple U6 structures. Ternary complex formation between U4_{WT}, U6_{WT}, and oligo A is shown in lane 5. **(B)** Complex formation between U4₁₋₆₄ and U6₂₅₋₁₁₂ (lane 1), U6_{MUT2} (lane 2), and U6_{MUT1} (lane 3). **(C)** Complex formation between U4₁₋₆₄ and U6₂₅₋₁₁₂ (lane 1), U6_{BASE} (lane 2), U6_{ΔBULGE} (lane 3), U6_{BASE+ΔBULGE} (lane 4), U6_{A34G/A35G} (lane 5), U6_{G96C/A97C} (lane 6), and U6_{G96C/A97C/U100C/U101C} (lane 7). Some of the stabilizing mutations cause different mobility on the native gel relative to WT consistent with alternate structures as seen in smFRET experiments.



Supplemental Figure 3. Probability density histogram of lifetimes for the low and high E_{FRET} states observed in $U4_{WT}/U6_{25-112}$ di-RNAs. Points represent bin centers of the histogram. Red lines represent fits of the distributions of lifetimes to equations described in the Materials and Methods. Fit parameters are shown in each box plot. **(A)** Histogram of low E_{FRET} state lifetimes for $U4_{WT}/U6_{25-112}$ ($N = 595$ events on 79 di-RNAs). **(B)** Histogram of high E_{FRET} state lifetimes for $U4_{WT}/U6_{25-112}$ ($N = 584$ events on 79 di-RNAs). **(C)** Histogram of low E_{FRET} state lifetimes for $U4_{1-64}/U6_{25-112}$ ($N = 772$ events on 80 di-RNAs). **(D)** Histogram of high E_{FRET} state lifetimes for $U4_{1-64}/U6_{25-112}$ ($N = 777$ events on 80 di-RNAs). **(E)** Histogram of high E_{FRET} state lifetimes for $U4_{1-64}/U6_{MUT1}$ ($N = 227$ events on 63 di-RNAs). **(F)** Histogram of high E_{FRET} state lifetimes for $U4_{1-64}/U6_{BASE}$ ($N = 143$ events on 74 di-RNAs). Error bars represent the error in counting statistics for each bin as calculated by the variance for a binomial distribution.

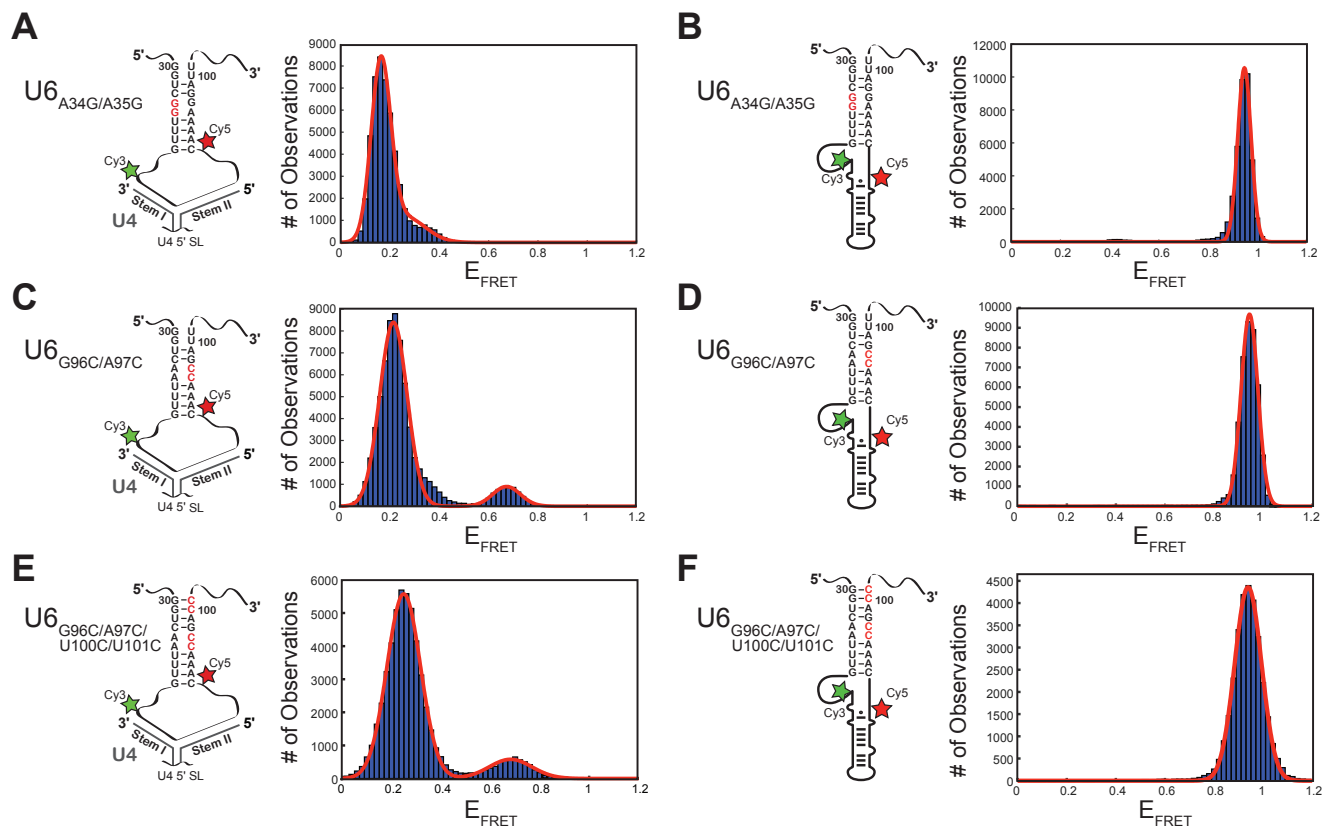


Supplemental Figure 4. Impact of monovalent and divalent cations on U4_{WT}/U6₂₅₋₁₁₂ smFRET dynamics. **(A)** Histogram of E_{FRET} values obtained from single molecules of U4_{WT}/U6₂₅₋₁₁₂ ($N = 141$) at 150 mM NaCl. The distribution could be fit to a single Gaussian function centered at 0.23 ± 0.01 (red line). **(B)** Histogram of E_{FRET} values obtained from single molecules of U4_{WT}/U6₂₅₋₁₁₂ ($N = 111$) at 400 mM NaCl. The distribution could be fit to a sum of two Gaussian functions centered at 0.25 ± 0.01 and 0.70 ± 0.01 (red line). **(C)** Histogram of E_{FRET} values obtained from single molecules of U4_{WT}/U6₂₅₋₁₁₂ ($N = 118$) at 150 mM NaCl, 10 mM MgCl₂. The distribution could be fit to a sum of two Gaussian functions centered at 0.25 ± 0.01 and 0.67 ± 0.01 (red line). **(D)** Histogram of E_{FRET} values obtained from single molecules of U4_{WT}/U6₂₅₋₁₁₂ ($N = 114$) at 400 mM NaCl, 10 mM MgCl₂. The distribution could be fit to a sum of two Gaussian functions centered at 0.25 ± 0.01 and 0.68 ± 0.01 (red line).



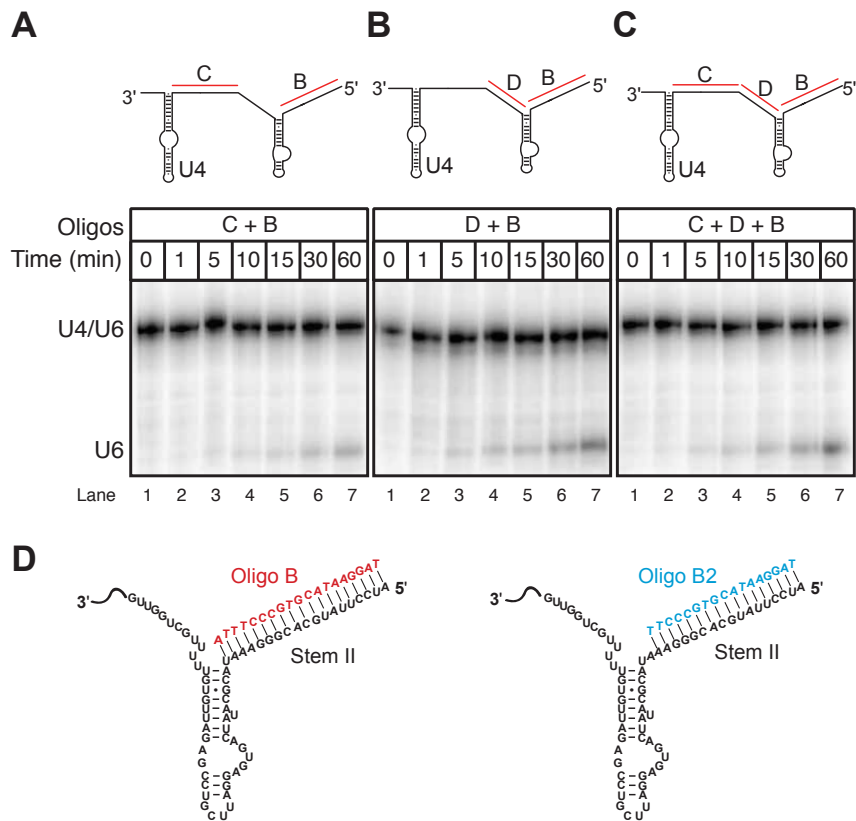
Supplemental Figure 5. U6 telestem mutants have the same E_{FRET} distribution as $U6_{\text{WT}}$ in the absence of U4. **(A, Left)** Cartoon of $U6_{\text{Mut1}}$ showing the location of the telestem mutation in red. **(A, Right)** Histogram of E_{FRET} values obtained from single

molecules of $U6_{Mut1}$ ($N = 68$). The distribution could be to a single Gaussian distribution centered at 0.96 ± 0.01 (red line). **(B, Left)** Cartoon of $U6_{Mut2}$ showing the location of the telestem mutation in red. **(B, Right)** Histogram of E_{FRET} values obtained from single molecules of $U6_{Mut2}$ ($N = 62$). The distribution could be to a single Gaussian distribution centered at 0.98 ± 0.01 (red line). **(C, Left)** Cartoon of $U6_{BASE}$ showing the location of the telestem mutation in red. **(C, Right)** Histogram of E_{FRET} values obtained from single molecules of $U6_{BASE}$ ($N = 74$). The distribution could be to a single Gaussian distribution centered at 0.95 ± 0.01 (red line). **(D, Left)** Cartoon of $U6_{\Delta BULGE}$ showing the location of the telestem mutation in red. **(D, Right)** Histogram of E_{FRET} values obtained from single molecules of $U6_{\Delta BULGE}$ ($N = 103$). The distribution could be to a single Gaussian distribution centered at 0.93 ± 0.01 (red line). **(E, Left)** Cartoon of $U6_{BASE+\Delta BULGE}$ showing the location of the telestem mutation in red. **(E, Right)** Histogram of E_{FRET} values obtained from single molecules of $U6_{BASE+\Delta BULGE}$ ($N = 102$). The distribution could be to a single Gaussian distribution centered at 0.94 ± 0.01 (red line).

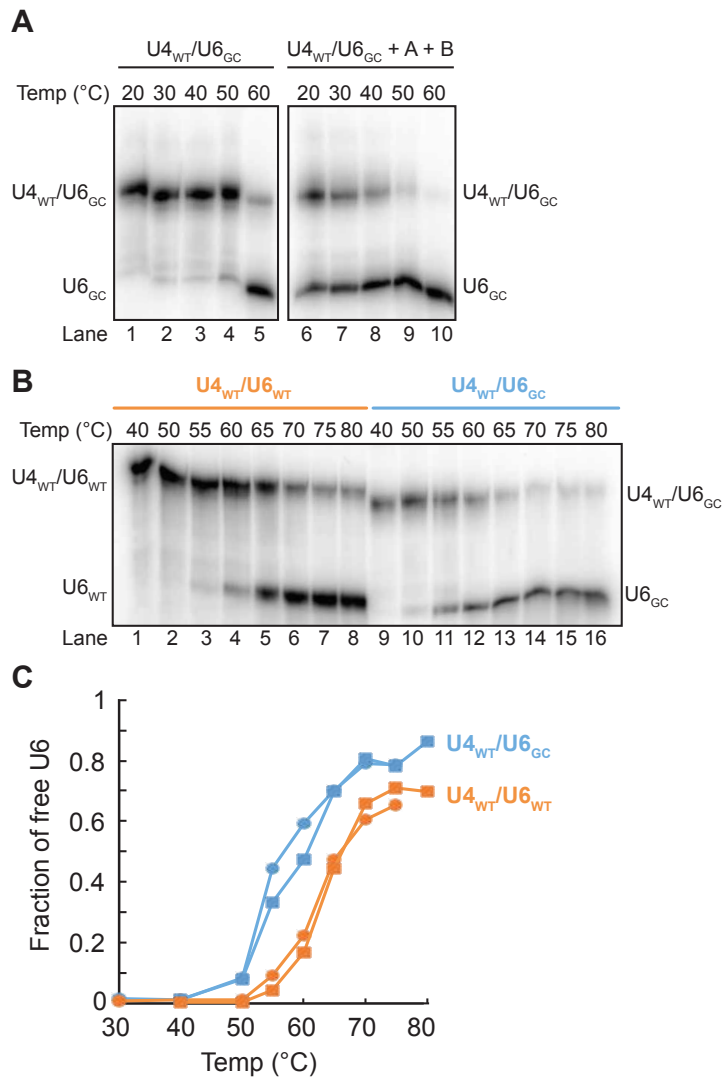


Supplemental Figure 6. Single strand mutations of the telestem stabilizing U6 RNAs used in smFRET experiments differentially influence the observed U4/U6 dynamics but do not impact FRET observed with U6 alone. **(A, Left)** Cartoon of U6_{A34G/A35G} showing the location of the telestem mutation in red. **(A, Right)** Histogram of E_{FRET} values obtained from single molecules of U6_{A34G/A35G} ($N = 108$). The distribution could be to the sum of two Gaussians centered at 0.16 ± 0.01 and 0.26 ± 0.06 (red line). **(B, Left)** Cartoon of U6_{G96C/A97C} showing the location of the telestem mutation in red. **(B, Right)** Histogram of E_{FRET} values obtained from single molecules of U6_{G96C/A97C} ($N = 114$). The distribution could be to the sum of two Gaussians centered at 0.21 ± 0.01 and 0.67 ± 0.02 (red line). **(C, Left)** Cartoon of U6_{G96C/A97C/U100C/U101C} showing the location of the telestem mutation in red. **(C, Right)** Histogram of E_{FRET} values obtained from single molecules of U6_{G96C/A97C/U100C/U101C} ($N = 100$). The distribution could be to the sum of

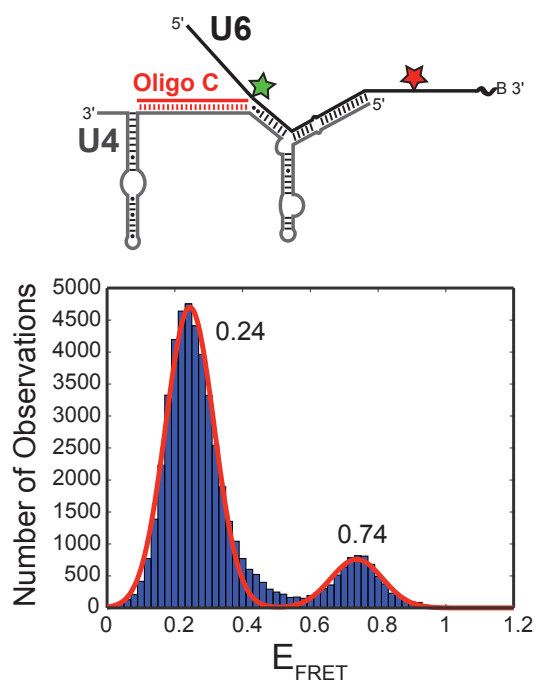
two Gaussians centered at 0.25 ± 0.01 and 0.68 ± 0.01 (red line). **(D, Left)** Cartoon of $U6_{A34G/A35G}$ showing the location of the telestem mutation in red. **(D, Right)** Histogram of E_{FRET} values obtained from single molecules of $U6_{A34G/A35G}$ ($N = 128$). The distribution could be to a single Gaussian distribution centered at 0.95 ± 0.01 (red line). **(E, Left)** Cartoon of $U6_{G96C/A97C}$ showing the location of the telestem mutation in red. **(E, Right)** Histogram of E_{FRET} values obtained from single molecules of $U6_{G96C/A97C}$ ($N = 104$). The distribution could be to a single Gaussian distribution centered at 0.95 ± 0.01 (red line). **(F, Left)** Cartoon of $U6_{G96C/A97C/U100C/U101C}$ showing the location of the telestem mutation in red. **(F, Right)** Histogram of E_{FRET} values obtained from single molecules of $U6_{G96C/A97C/U100C/U101C}$ ($N = 106$). The distribution could be to a single Gaussian distribution centered at 0.94 ± 0.01 (red line).



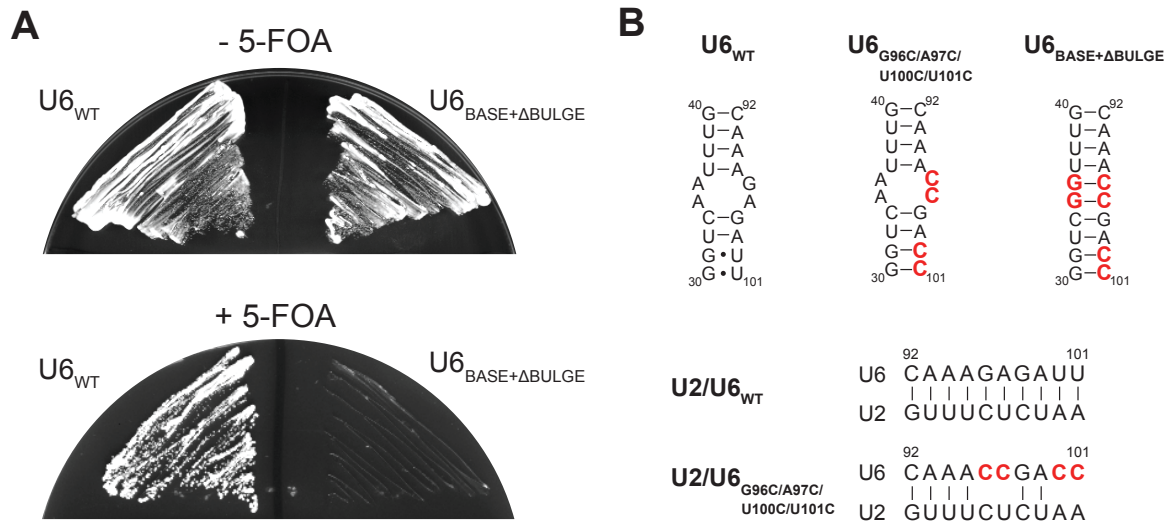
Supplemental Figure 7. Oligos incapable of both forming a toehold on U4 and strand invasion of U4/U6 stem I do not support rapid U4/U6 unwinding when mixed with unwinding oligo B. **(A)** Unwinding observed upon mixing U4_{WT}/U6_{WT} with oligos B and C, which binds the ssRNA region of U4 to create a toehold but is incapable of strand invasion of stem I. Replicate experiments were used to obtain a fitted unwinding rate of $0.011 \pm 0.007 \text{ min}^{-1}$. **(B)** Unwinding observed upon mixing U4_{WT}/U6_{WT} with oligos B and D, which binds stem I but is incapable of forming a toehold. Replicate experiments were used to obtain a fitted unwinding rate of $0.005 \pm 0.003 \text{ min}^{-1}$. **(C)** Unwinding observed upon mixing oligos B, C, and D with U4_{WT}/U6_{WT}. Replicate experiments were used to obtain a fitted unwinding rate of $0.018 \pm 0.008 \text{ min}^{-1}$. **(D)** Difference between oligo B and B2 in binding to U4 RNA. Oligo B2 is two nucleotides shorter near the three-helix junction.



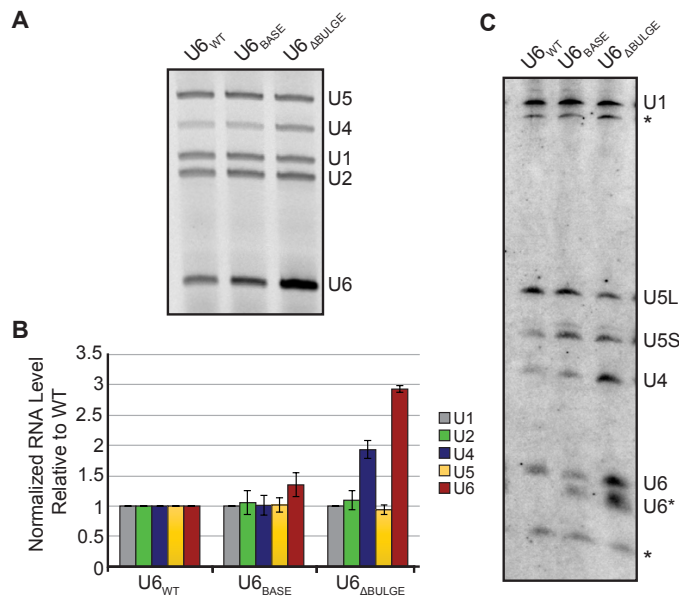
Supplemental Figure 8. U4_{WT}/U6_{GC} undergoes unwinding at a lower temperature than U4_{WT}/U6_{WT} in the presence and absence of oligos A and B. **(A)** U4_{WT}/U6_{GC} was diluted to 25 nM in annealing buffer with 400 mM NaCl in the absence (Lanes 1-5) or presence (Lanes 6-10) of oligos A and B and then incubated at the indicated temperatures for 10 min. Samples were then analyzed by nondenaturing PAGE **(B)** U4/U6 unwinding was followed in the absence of oligos at temperatures from 40-80°C following procedures described in (A). **(C)** Quantification of the data shown in (B) along with an additional replicate. U4_{WT}/U6_{GC} forms a larger amount of free U6 at temperatures above 40°C than does U4_{WT}/U6_{WT}.



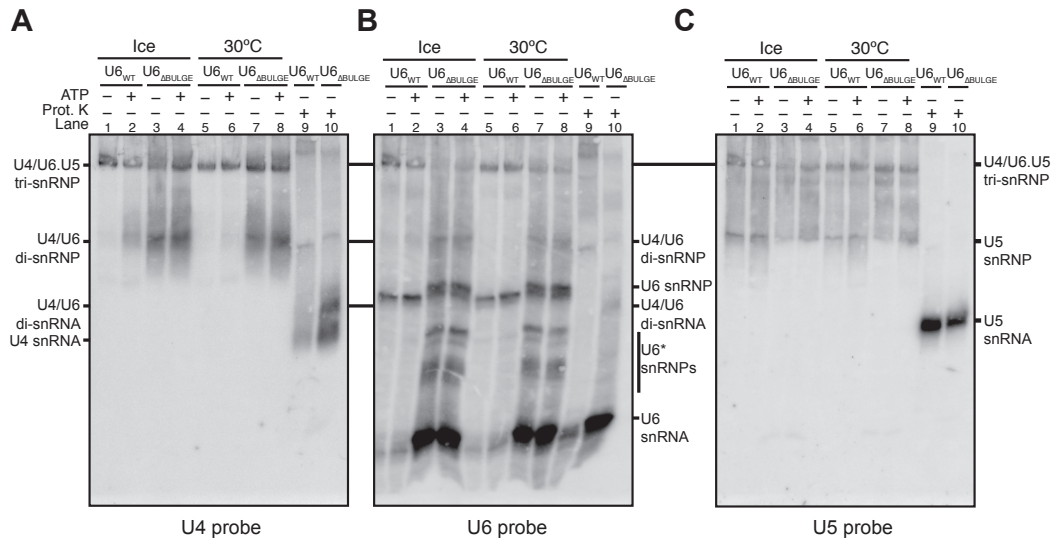
Supplemental Figure 9. Oligo C does not induce formation of new E_{FRET} states in $U4_{\text{WT}}/U6_{25-112}$. (Top) Cartoon of the oligo C/ $U4_{\text{WT}}/U6_{25-112}$ ternary complex. (Bottom) Histogram of E_{FRET} values obtained from single molecules of oligo C/ $U4_{\text{WT}}/U6_{25-112}$ ($N = 90$). The distribution could be fit to a sum of two Gaussian functions centered at 0.24 ± 0.01 and 0.74 ± 0.02 (red line).



Supplemental Figure 10. U6_{BASE+ΔBULGE} is not viable after 5-FOA selection at 30°C. (A) Shown are photographs of single colonies of yeast streaked onto –TRP, –HIS dropout plates that either lack (top) or contain (bottom) 5-FOA. Yeast were transformed with plasmids encoding U6_{WT} or U6_{BASE+ΔBULGE}, along with U4_{WT}. (B) Secondary structure comparison between the U6 telestem and U2/U6 helix II. The 3' strand mutations, in particular, the U6_{G96C/A97C/U100C/U101C} mutation, destabilize U2/U6 helix II.



Supplemental Figure 11. Analysis of RNA levels in U6_{WT}, U6_{BASE}, and U6_{ΔBULGE} strains. **(A)** Primer extension of total cellular RNA isolated from indicated yeast strains using Cy5-labeled primers against U1, U2, U4, U5 and U6. **(B)** Quantification of primer extension analysis for each snRNA. Each RNA level was normalized to U1 RNA level to account for any differences in the amount of total RNA present in the primer extension reaction. Plotted is the average of three biological replicates relative to U6_{WT} and error bars represent the standard deviation. **(C)** Northern blot of total cellular RNAs isolated from indicated yeast strains and probed with [³²P]-labeled oligos complementary to the U1, U4, U5, and U6 snRNAs. An equivalent amount of RNA (5 μg) was loaded in each lane. U6* indicates smaller U6 snRNAs. Asterisks represent uncharacterized RNA species appearing below U1 and U6 when probed with oligos complementary to U4 and U6, respectively.



Supplemental Figure 12. Uncropped image of the native Northern blot from Figure 7 in the main text. The extracts were incubated either at 30°C or on ice prior to electrophoresis. The difference in snRNP distribution between the two incubation procedures is minimal.

Supplemental Table 1. Fluorescent U6 RNAs for smFRET

Construct	Sequence
5' FRAG U6 ₂₅₋₁₁₂ (U54)	5' - AUUUGGUCAAUUUGAAACAAUACAGAGA/ <i>iAmMC6T</i> /GAUCA GCAGUCCCCUGCAU - 3'
3' FRAG U6 ₂₅₋₁₁₂ (U90)	5' - AAGGAUGAACCGUUU/ <i>iAmMC6T</i> /ACAAAGAGAUUUUUUUUCGU UUUGUCUUCUAUUUAAUUUUUCCC/3'BIO/ - 3'
5' FRAG U6 ₂₅₋₁₁₂ (U46)	5' - AUUUGGUCAAUUUGAAACAA/ <i>iAmMC6T</i> /ACAGAGAUGAUCAG CAGUCCCCUGCAU - 3'
5' FRAG U6 _{MUT1} (U54)	5' - AUUUUUCGAAUUUGAAACAAAUCAGAGA/ <i>iAmMC6T</i> /GAUCAG CAGUCCCCUGCAU - 3'
5' FRAG U6 _{MUT2} (U54)	5' - AUUUGGUCAA GGCC AAACAAUACAGAGA/ <i>iAmMC6T</i> /GAUCAG CAGUCCCCUGCAU - 3'
3' FRAG U6 _{BASE} (U90)	5' - AAGGAUGAACCGUUU/ <i>iAmMC6T</i> /ACAAAGAGAC CC UAUUUUCGU UUUGUCUUCUAUUUAAUUUUUCCC/3'BIO/ - 3'
5' FRAG U6 _{ΔBULGE} (U54)	5' - AUUUGGUC GG UUUGAAACAA/ <i>iAmMC6T</i> /ACAGAGAUGAUCAG CAGUCCCCUGCAU - 3'
3' FRAG U6 _{ΔBULGE} (U90)	5' - AAGGAUGAACCGUUU/ <i>iAmMC6T</i> /ACAA CC GAUUUUUUUCGU UUUGUCUUCUAUUUAAUUUUUCCC/3'BIO/ - 3'
3' FRAG U6 _{ΔBULGE+BASE} (U54)	5' - AAGGAUGAACCGUUU/ <i>iAmMC6T</i> /ACAA CCGACC UAUUUUCGU UUUGUCUUCUAUUUAAUUUUUCCC/3'BIO/ - 3'
U6 ligation DNA splint	5' – CTCTTTGTAAAACGGTTCATCCTTATGCAGGGGAACTGCTGAT CATCTCTGTATTG - 3'

C6-aminoallyl modifications are indicated with /iAmMC6T/ with colors indicating either Cy3 (green) or Cy5 (red) labeling. Mutations in the U6 RNA are highlighted in blue.

Supplemental Table 2. Nucleotide sequences of nonfluorescent RNAs

Construct	Sequence
U4 _{WT}	5' – GGAUCCUUAUGCACGGGAAAUACGCAUAUCAGUGAG GAUUCGUCCGAGAUUGUGUUUUUGCUGGUUGAAAUUUAU UAUAAACCAGACCGUCUCCUCAUGGUCAAUUCGGUGUUCG CUUUUGAAUACUUCAAGACUAUGUAGGGAAUUUUUGGAU ACCUUU - 3'
U4 ₁₋₆₄	5' – GGAUCCUUAUGCACGGGAAAUACGCAUAUCAGUGAGG AUUCGUCCGAGAUUGUGUUUUUGCUGGUU - 3'
U4 ₁₋₅₅	5' – GGAUCCUUAUGCACGGGAAAUACGCAUAUCAGUGAGG AUUCGUCCGAGAUUGUGUUU - 3'
U6 _{WT}	5' – GGUUCGCGAAGUAACCCUUCGUGGACAUUUGGUCAA UUUGAAACAAUACAGAGAUGAUCAGCAGUCCCCUGCAUA AGGAUGAACCGUUUUACAAAGAGAUUUUUAUUUCGUUUU - 3'
U6 _{GC}	5' – GGUUCGCGAAGUAACCCUUCGUGGACAUUUGG CCGG UUUGAAACAAUACAGAGAUGAUCAGCAGUCCCCUGCAUA AGGAUGAACCGUUUUACAA CCGGCC UAUUUCGUUUU - 3'
U6 ₄₉₋₈₈	5' - AGAGA/iAmMC6T/GAUCAGCAGUCCCCUGCAUAAGGA UGAACCGU - 3'

GC substitutions in U6_{GC} are shown in red.

Supplemental Table 3. DNA oligos used for U4/U6 unwinding assays

Oligo name	Sequence	Notes
A	5' – GACGGTCTGGTTTATAATTAATTTC AACCAGCAA - 3'	Complementary to U4 nts 56-91
B	5' - ATTTCCCGTGCATAAGGAT - 3'	Complementary to U4 nts 1-19
B2	5' - TTCCCGTGCATAAGGAT - 3'	Complementary to U4 nts 1-17
C	5' - GACGGTCTGGTTTATAATTAATTT - 3'	Complementary to U4 nts 66-91
D	5' - CAACCAGCGGGAA - 3'	Complementary to U4 nts 53-65

Supplemental Table 4. Plasmids used in this study

Plasmid ID	Common Name	Description
pAAH0413	pRS313-U4 _{WT}	HIS3/CEN encoding U4 _{WT}
pAAH0412	pRS314-U6 _{WT}	TRP1/CEN encoding U6 _{WT}
pAAH0428	pRS314-U6 _{A34G/A35G}	TRP1/CEN encoding U6 _{A34G/A35G}
pAAH0429	pRS314-U6 _{G96C/A97C}	TRP1/CEN encoding U6 _{G96C/A97C}
pAAH0430	pRS314-U6 _{BASE}	TRP1/CEN encoding U6 _{BASE}
pAAH0702	pRS314-U6 _{ΔBULGE}	TRP1/CEN encoding U6 _{ΔBULGE}
pAAH0704	pRS314-U6 _{G96C/A97C/U100C/U101C}	TRP1/CEN encoding U6 _{G96C/A97C/U100C/U101C}
pAAH0703	pRS314 _{BASE+ΔBULGE}	TRP1/CEN encoding U6 _{BASE+ΔBULGE}

Plasmids pAAH0413, and pAAH0412 have been previously described by McManus *et al.* (1).

Supplemental Table 5. Yeast strains used in this study

Strain ID	Genotype	Description
CJM000	<i>MATa, snr6::LEU2, snr14::trp1::ADE2, trp1, ura3, lys2, his3, ade2</i> [pRS316-U4wt-U6mini]	Shuffle strain for U4 and U6
yAAH0431	CJM000 + pAAH0413 + pAAH0412	Strain expressing U4 _{WT} , U6 _{WT}
yAAH1552	CJM000 + pAAH0413 + pAAH0428	Strain expressing U4 _{WT} , U6 _{A34G/A35G}
yAAH1553	CJM000 + pAAH0413 + pAAH0429	Strain expressing U4 _{WT} , U6 _{G96C/A97C}
yAAH0432	CJM000 + pAAH0413 + pAAH0430	Strain expressing U4 _{WT} , U6 _{BASE}
yAAH1554	CJM000 + pAAH0413 + pAAH0702	Strain expressing U4 _{WT} , U6 _{ΔBULGE}
yAAH1555	CJM000 + pAAH0413 + pAAH0704	Strain expressing U4 _{WT} , U6 _{G96C/A97C/U100C/U101C}
--	CJM000 + pAAH0413 + pAAH0703	Not Viable

Strain CJM000 has been previously described by McManus *et al.* (1).

Supplemental Table 6. Probes for solution hybridization and Northern blotting

Probe	Sequence	Description
U1-SH	5' – CCGTATGTGTGTGTGACC – 3'	Used for solution hybridization and native northern analysis
SR-U2	5' – CAGATACTACACTTG – 3'	Used for native northern analysis
U4-14b	5' – AGGTATTCCAAAAATTCCC – 3'	Used for solution hybridization and native northern analysis
U5B	5' – AAGTTCCAAAAAATATGGCAAGC – 3'	Used for native northern analysis
U6-SH	5' – ATTGTTTCAAATTGACCAAAT – 3'	Used for solution hybridization and native northern analysis
U6-SH-MUT	5' – ATTGTTTCAAACCGACCAAAT – 3'	Used for solution hybridization and native northern analysis
U1-Long	5' – GATCAGTAGGACTTCTTGATCTCCTC TGATATCTTAAG – 3'	Used for denaturing northern analysis
U4-Long	5' – GCAAAAACACAATCTCGGACGAATCC TCACTG – 3'	Used for denaturing northern analysis
U5-Long	5' – GCAAGAACCATGTTTCGTTATAGTTCT ATAGGC – 3'	Used for denaturing northern analysis
U6-Long	5' – CCAAATGTCCACGAAGGGTACTTCG CGAAC – 3'	Used for denaturing northern analysis

Probes for solution hybridization and native northern analysis were obtained from Burke et al. and references therein (2).

Supplemental Table 7. Fluorescent primers used for primer extension

Primer	Sequence
Cy5_U1RT136	5' – /5Cy5/GACCAAGGAGTTTGCATCAATGAC – 3'
XC5	5' – /5Cy5/TTTGGGTGCCAAAAAATGTGTATTGTAAC – 3'
XC6	5' – /5Cy5/GGTATTCCAAAAATCCCTACATAGTC – 3'
XC7	5' – /5Cy5/AAGTTCCAAAAATATGGCAAGC – 3'
XC9	5' – /5Cy5/TCATCCTTATGCAGGGGAACTG – 3'

Primer extension primers were adapted from McGrail et al. (3).

Supplemental References

1. McManus, C.J., Schwartz, M.L., Butcher, S.E. and Brow, D.A. (2007) A dynamic bulge in the U6 RNA internal stem-loop functions in spliceosome assembly and activation. *RNA*, **13**, 2252–2265.
2. Burke, J.E., Butcher, S.E. and Brow, D.A. (2015) Spliceosome assembly in the absence of stable U4/U6 RNA pairing. *RNA*, **21**, 923–934.
3. McGrail, J.C., Krause, A. and O'Keefe, R.T. (2009) The RNA binding protein Cwc2 interacts directly with the U6 snRNA to link the nineteen complex to the spliceosome during pre-mRNA splicing. *Nucleic Acids Research*, **37**, 4205–4217.